

Biomass and Lipid Production by *Pseudochloris wilhelmii* in Sea-Wastewater Mixtures: Modeling and Experiments

Alessandro Concas^{a*}, Giovanni Antonio Lutz^b, Massimo Pisu^a, Giacomo Cao^{b,c}

^aCenter for Advanced Studies, Research and Development in Sardinia (CRS4), Loc. Piscina Manna, Building 1, 09050 Pula (CA), Italy

^bInterdepartmental Center of Environmental Science and Engineering (CINSA), University of Cagliari, Via San Giorgio 12, 09124 Cagliari, Italy

^cDepartment of Mechanical, Chemical and Materials Engineering, University of Cagliari, Via Marengo 2, 09123 Cagliari, Italy
aconcas@crs4.it

The microalga *Pseudochloris wilhelmii* was cultivated in low-cost media consisting of mixtures of seawater and wastewaters simulants. Under specific conditions, the strain was capable to grow while synthesizing good quality lipids. In fact, FAMES composition of lipids was such to potentially permit producing a viable biodiesel. A mathematical model was developed to simulate the dynamics of biomass and nutrients concentration as well as lipid content and pH. The model was then validated by comparison with the experimental results.

1. Introduction

Production of biofuels from microalgae is still expensive due to the high costs of cultivation, harvesting and lipid extraction steps (Abinandan et al., 2018). A possible solution to reduce costs associated to replenishment of water and nutrients is to exploit seawater as costless resource to obtain micronutrients (Ummalyma et al., 2018). Different wastewaters (WWs) could be also used as inexpensive source of nitrogen (N) and phosphorus (P) (Lutz et al., 2021). Hence, a suitably tuned mixture of seawater (SW) and secondary WW could be employed as a low-cost growth medium in the process for producing microalgae biofuels. In this regard, the marine green alga *Pseudochloris wilhelmii* (PW) can produce quite good amounts of lipids under specific operating conditions (Lutz et al., 2015). A process where a SW-secondary WW is used as culture medium can be constrained by the optimization of the microalgae cultivation system in terms of design, operation, and control. This aspect could be overcome by using suitable mathematical models that are capable to quantitatively describe the effects of crucial operating parameters such as light intensity, pH, mass transfer conditions and growth medium composition. Mathematical tools to simulate pH evolution and its effect on growth are particularly useful for the optimization of microalgae-based processes especially when they involve pH-sensitive strains such as PW (Concas et al., 2019). To the best of our knowledge, only the model by Concas et al. (2013) was capable to simulate and predict the effect of a high number of ionic equilibria on the final pH by relying on the electro-neutrality condition. However, this approach can be exploited only when the composition of growth medium is well known, and the kinetics parameters of the strain are available. Alternative methods to predict pH of the solution are needed when considering the cultivation of pH-sensitive microalgae (in particular new strains such as PW) in WWs. Therefore the aim of this work is to present, for the first time, a novel comprehensive model where the evolution of biomass, lipid and pH during the cultivation of PW in low-cost media (involving WWs) are predicted by taking into account the effect of all the ionic species in solution without their respective kinetic parameters being known.

2. Materials and methods

2.1 Microorganism and seed culture medium

PW (SAG strain 55.87) was provided by the University of Göttingen, Germany. Stock cultures were propagated and maintained in Erlenmeyer flasks in Brackish Water Medium (BWM), under incubation conditions of 25°C. The BWM was prepared according to Lutz et al. (2012) without using soil extract. During the incubation period

a photon flux density of $98 \mu\text{mol m}^{-2} \text{s}^{-1}$ was assured by four 15 W white fluorescent tubes and a light/dark photoperiod of 12 h was imposed. Flasks were subjected to a continuous shaking at 100 rpm (Universal Table Shaker 709).

2.2 Growth media

Low-cost media to grow PW were suitable mixtures of SW and municipal wastewater simulants (SWW). Volumetric mixing ratio of SW to SWWs was set to 1:1. Mediterranean SW (lat. $39^\circ 11' \text{ N}$ - long. $09^\circ 10' \text{ E}$) was collected, then sterilized through an autoclave (Thermo Fisher Scientific Inc.) and finally filtered by means of $0.45 \mu\text{m}$ filter. Two different SWW were prepared and subsequently mixed with the SW. The first one, SWW-A, was obtained by slightly modifying the composition proposed by Wang et al. (2009) while the second one, SWW-B, was prepared by slightly changing that one suggested by Ghangrekar and Scinde (2006). In both cases, organic carbon sources were not considered in order to prevent bacterial contamination. This way, simulants of secondary WWs, obtained as result of secondary treatments ideally characterized by 100% removal yields of dissolved organic carbons (DOC), were considered. After mixing with SW, two low-cost growth media, named LCM-A and LCM-B, were obtained. The media composition has been reported in Concas et al. (2019).

2.3 Cultivation of microalgae

Growth experiments were carried out in a cylindrical glass photobioreactor (PBR), having 9.5 cm diameter and 21 cm height as dimensions, a volume of 1.5 L and was operated in semi batch configuration, i.e. batch for the liquid phase and continuous mode for the gas one, respectively. Culture media were sterilized in autoclave at 121°C for 20 min prior to microalgae inoculation. The initial cell concentration in each experiment varied within the range $0.01 - 0.02 \text{ g L}^{-1}$. The PBR was then filled with 1 L of growth medium and stirred at 400 rpm using a rotating blade powered by an electrical engine. During the experiments, cultures were maintained at 25°C by means of a thermostatic bath (GD120 series) and illuminated using a photon flux density of $100 \mu\text{mol m}^{-2} \text{s}^{-1}$, provided by eight 11 W white fluorescent lamps with a light/dark photoperiod of 12 h. Configuration of lamps has been reported elsewhere (Concas et al., 2013). Atmospheric air was continuously supplied through suitable spargers at flowrate of 125 mL min^{-1} using a pump (Air 550 R plus). Each experiment was performed at least twice for the sake of reproducibility.

2.4 Biomass and pH measurements

Microalgae growth was monitored through daily measurements of the optical density at 560 nm wavelength (OD_{560}) of the culture media by means of a suitable spectrophotometer (Genesys 20 spectrophotometer, Thermo Fisher Scientific Inc.). Calculation of biomass concentration has been reported elsewhere (Lutzu et al. 2012). The pH was measured daily by means of a pHmeter (KNICK 913). Each measure of both OD and pH was performed at least twice for the sake of reproducibility.

2.5 Lipid extraction and fatty acid methyl esters analysis

Cell disruption was performed through Fenton reaction, and the subsequent neutral lipid extraction was performed directly on disrupted wet biomass through ethanol and hexane according to a method described elsewhere (Concas et al., 2019). Total amount of saponifiable lipids and fatty acid composition of extracted lipid were determined after transesterification with methanol-acetyl chloride. Gas chromatographic analysis was carried out according to European Regulation N° 2568/91 using a flame ionization detector (Thermo Trace Ultra, GC-14B) and a RTX-WAX column T (fused silica, $0.25 \text{ mm} \times 60 \text{ m} \times 0.25 \mu\text{m}$) maintained at 180°C . Helium was used as carrier gas at a rate of 1 mL min^{-1} . Analysis of the fuel properties of the biodiesel obtainable from the extracted lipids was performed based on the fatty acids methyl esters (FAME) composition through the software Biodiesel Analyzer© Ver. 2.2 (Concas et al., 2016b).

3. Mathematical model

Considering isotherm conditions and the fact that limiting factors affecting microalgae growth during the experiments were light intensity, nutrient's concentration, and medium pH, respectively, the mass balance for the functional (non-lipidic) microalgae biomass in the batch PBR can be written as shown in Eq.1:

$$\frac{dC_x}{dt} = \mu_{\max} \left(\prod_{j=1}^n \frac{[C_j]}{[C_j] + K_j} \right) \cdot \left(\frac{I_{av}}{I_{av} + I_{K,h} + \frac{I_{av}^2}{I_{K,i}}} \right) \cdot \left(\frac{\frac{k_0}{k_1} + \frac{1}{K_1} [H^+] + \frac{k_2}{k_1 K_1 K_2} [H^+]^2}{1 + \frac{1}{K_1} [H^+] + \frac{1}{K_1 K_2} [H^+]^2} \right) \cdot C_x - \mu_d \cdot C_x \quad (1)$$

along with the initial condition $C_x = C_x^0$ at $t = 0$. In Eq.1, the symbol C_x represents the non-lipidic fraction of biomass while C_j with $j = TIC, TIN, TIP$ is the bulk concentration of total inorganic carbon (TIC), nitrogen (TIN) and phosphorus (TIP). The terms within parentheses represents the dependence of the growth rate upon the

limiting factors that were nutrients, average light intensity within the culture I_{av} , and culture pH, respectively (Concas et al., 2019). The kinetic dependence of growth rate on light intensity I_{av} , considered in the second factor within parentheses, was evaluated according to Concas et al. (2016a). The effect of pH, in the third factor was instead evaluated with relationship proposed by Tan et al. (1998). The growth rate thus depends upon TIC in the liquid bulk which, in turn, is affected by CO₂ mass transfer from the gas phase and consumption by algae. Accordingly, the following mass balance holds true for TIC:

$$V_L \frac{d[C_{TIC}]}{dt} = V_R k_L a (H_{CO_2} [C_{g,CO_2}] - [C_{L,CO_2}]) - Y_{TIC} \frac{dC_X}{dt} V_L \quad (2)$$

along with the initial condition $C_{TIC} = C_{TIC}^0$ at $t = 0$. In Eq. 2, V_L and V_R represent the liquid and reactor volumes, respectively, while $k_L a$ is the mass transfer coefficient multiplied by the specific area of bubbles and Y_{TIC} is the TIC yield of biomass. The evolution of CO₂ concentration in the gas phase was evaluated through the following mass balance.

$$V_g \frac{d[C_{g,CO_2}]}{dt} = Q_g [C_{g,CO_2}^f] - Q_g [C_{g,CO_2}] - V_R k_L a (H_{CO_2} [C_{g,CO_2}] - [C_{L,CO_2}]) \quad (3)$$

along with the initial condition $[C_{g,CO_2}] = y_{CO_2} P_{air} / RT$ at $t = 0$ with y_{CO_2} representing the molar fraction of CO₂ in the gas phase bubbled into the liquid medium. The relationship between the liquid concentration of CO₂, (C_{L,CO_2}) and the total inorganic carbon (C_{TIC}) in the liquid phase was evaluated by considering that, at the gas-liquid interphase CO₂ first dissolves in the liquid bulk and then give rise to the chemical equilibria leading to the production of HCO₃⁻ and CO₃²⁻. By considering all these equilibrium relationships as well the electroneutrality of solution and following the approach proposed by Concas et al. (2013, 2019) it was possible to evaluate the pH of solution time by time as follows:

$$[H^+] = \frac{K_w}{[H^+]} + K_C \frac{[H^+]^2 [C_{TIC}]}{\psi([H^+])} + 2K_{2C} K_{1C} K_C \frac{[C_{TIC}]}{\psi([H^+])} + [Alk] \quad (4)$$

Where the symbol K represent the equilibrium constants of water (K_w), carbonic acid (K_C), bicarbonates (K_{1C}) and carbonates (K_{2C}) formation. The symbol Alk instead represents the non-carbonatic alkalinity of the medium and was demonstrated by Concas et al. (2019) to vary as a function of algae concentration according to Eq. 5:

$$\frac{d[Alk]}{dt} = Y_{Alk} \frac{dC_X}{dt} \quad (5)$$

Which can be solved along with the initial condition $[Alk] = [Alk]^0$ at $t = 0$ where $[Alk]^0$ is calculated imposing the known initial values $[H^+] = [H^+]^0$ and $[C_{TIC}] = [C_{TIC}]^0$ in Eq. (4) and solving it with respect to $[Alk]$. The consumption of limiting nutrients such as TIN and TIP was evaluated through the following mass balances:

$$\frac{d[C_j]}{dt} = -Y_j \frac{dC_X}{dt} \cdot \theta(I_{av}) \quad (6)$$

Along with the initial condition $[C_j] = [C_j]^0$ at $t = 0$ with $j = TIN, TIP$. The function $\theta(I_{av})$, taking into account that nutrients are consumed only when the light is on, is equal to 1 when $I_{av} > 0$ and equal to 0 when $I_{av} = 0$. Finally, lipid production was evaluated through the classical model for cell product formation as follows:

$$\frac{dC_L}{dt} = Y_L \frac{dC_X}{dt} + \beta_L C_X \quad (7)$$

along with the initial condition $[C_L] = [C_L]^0$ at $t = 0$. Finally, once the resulting ODEs system was solved, the total biomass concentration was evaluated time by time as $C_B = C_X + C_L$ while the percent weight content of lipid was calculated as $q_L = C_L / C_B$.

4. Results and Discussion

In Figure 1 the experimental obtained with the LCM-A and LCM-B media are shown in terms of biomass and lipid evolution in time. Referring to LCM-A, the culture started growing exponentially without a detectable lag phase until about 240 h (~ 10 days), when a decelerating growth of PW, underlined by the change of slope, took

place (Fig. 1a). The experiment was then stopped when biomass concentration achieved the value of about 0.35 g L⁻¹. It should be noted that the interruption occurred before the achievement of steady state because all the relevant information on process feasibility could be inferred by combining experimental and model results achieved up to 550 h of cultivation.

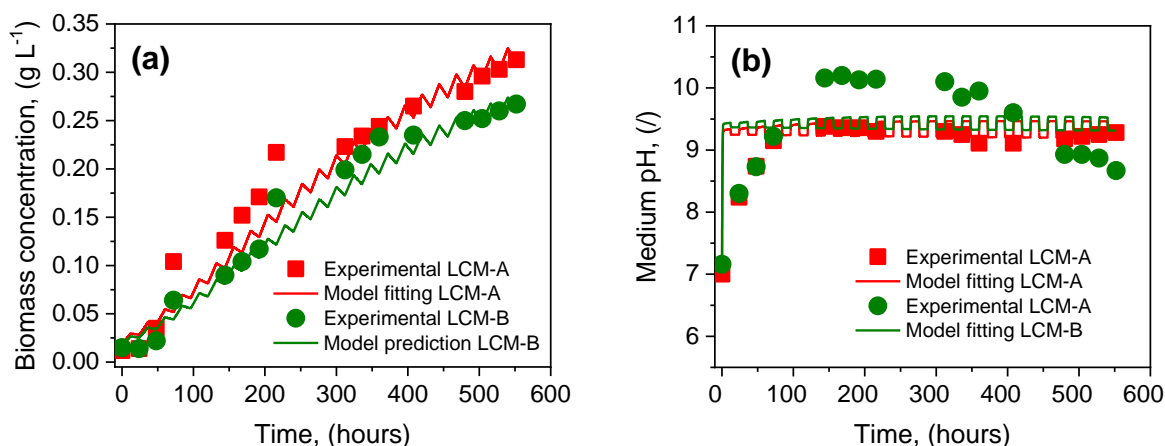


Figure 1. Comparison between experiments and model results in term of biomass (a) and pH (b) evolution.

The pH in LCM-A experiment, by starting from a value of about 7.0, increased abruptly in the first instants of cultivation and then achieved a kind of steady state at a value oscillating between 9.2 and 9.4. The sudden rise of pH was probably due to the Na₂HCO₃ already contained in the medium which caused the dissolved CO₂ to overcome the value that would have been in equilibrium with the CO₂ of the gas phase (air) fed to the reactor. Hence, the mass transfer of CO₂ occurred from the liquid phase to gas one leading to a drastic decrease of dissolved inorganic carbon and the consequent increase of pH. Subsequently, the CO₂ transferred in the opposite direction, i.e. from the gas to the liquid where it was consumed by microalgae thus leading the pH to achieve a kind of plateau. Data related to LCM-A are well fitted by model results (Fig. 1), in terms of both biomass and pH evolution, when the parameters are suitably adjusted to the values reported by Concas et al. (2019). The only difference lies in that the experiment showed a slightly less abrupt increase of pH during the first cultivation hours probably due to transitory effects neglected by the model, such as bubble formation and preferential gas pathways. To test the predictive capability of the model and the reliability of the parameter values by Concas et al. (2019), the experimental results obtained with the LCM-B were simulated without tuning any model parameter. Difference lies in the fact that biomass concentration in LCM-B achieved slight lower values than in LCM-A (Fig. 1a) due to the lower availability of N and P in the former which, in turn, resulted in lower growth rate of PW (Concas et al., 2019). However even the higher pH (pH~10.3) achieved in solution with LCM-B (Fig.1b) contributed to this difference. In fact, according to the pH-dependent kinetics in Eq. 1, higher pH values are capable to limit growth rate of PW in a stronger fashion with respect to the case of LCM-A experiments where pH achieved maximum values of 9.3 were obtained. The higher pH achieved in LCM-B are probably due to a more efficient photosynthesis (that consumes CO₂) of PW in this medium. As it can be seen from Fig.1, even the experimental data obtained with LCM-B, very similar to the ones obtained with the LCM-A, are well predicted by the proposed model that thus confirms its consistency. Only in the range of time from 150 to 350 h the agreement between model and experiments is not so good probably because of phenomena occurring neglected by model equations. However, before and after this period the model well captures the experimental behavior even in terms of pH evolution. Thus, it can be stated that the model represents a useful tool to extrapolate key information about the feasibility of using these LCM from cultivating PW at larger scales. To this aim, also the knowledge of lipids contents as well as of productivities achievable with the investigated systems (PW + LCM) is crucial.

Lipid content achieved at the end of cultivation when using the LCM-A was equal to about 17.3 %wt while it was equal to 17.1 %wt with LCM-B (Fig. 2a). As far the biomass productivity achieved at the end of the batch operation of PBRs was about 13 and 11 g m⁻³ d⁻¹ for the experiments with LCM-A and LCM-B, respectively (Fig. 2a). As above mentioned, this was probably due to the higher content of nutrients in LCM-A than LCM-B. Multiplication of biomass productivity by the lipid content allowed evaluating the lipid productivity which resulted to be 2.2 and 1.8 g m⁻³ d⁻¹ for LCM-A and LCM-B, respectively (Fig. 2a). While the above values are apparently relatively low, it should be stressed here that they were obtained by interrupting the experiments before the steady state was achieved, i.e when the cultures were still growing. Therefore, they are susceptible of significant increases. In Fig. 2b the composition of FAMES analyzed after transesterification of lipids extracted from PW

cultivated is shown. Palmitic acid (C16:0), oleic acid (C18:1) and linoleic acid (C18:2), i.e. the typical components of valuable biodiesels, were the prevalent FAMES whatever the LCM considered. The cumulative amounts of FAMES with carbon numbers from C16 to C18 were equal to 73 %wt and 84 %wt for the experiments with LCM-A and LCM-B, respectively.

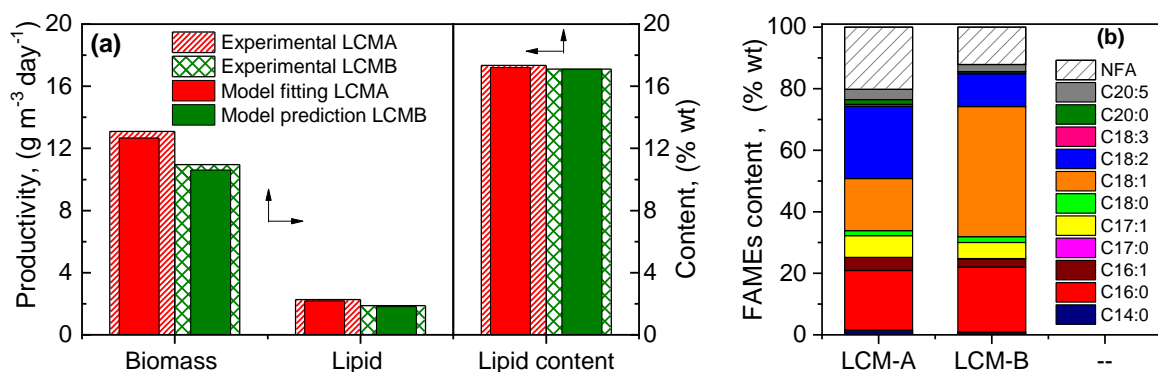


Figure 2. Comparison of experimental and simulated productivities (left Y axis) and lipid content (right Y axis) obtained with the investigated media (a) and fatty acids methyl esters composition of extracted lipids (b).

Nevertheless, C18:1, which is the most desirable FAME for biodiesel production, was much higher (~42 %wt) in the lipids obtained from the algae cultivated with the LCM-B medium. In contrast, lipids extracted from PW cultivated in LCM-A showed a higher relative content of the unsaturated forms of C18 with more than one double bonds, i.e. C18:2 and C18:3. The possibility of using the extracted lipids for producing biodiesel was further evaluated on the basis of the FAMES profiles by taking advantage of the software Biodiesel Analyzer® Ver. 2.2. The results of such analysis are reported in Table 1 only with reference to the parameters for which specific prescriptions of international standards existed (Table 1).

Table 1. Composition of biodiesels obtainable from lipids extracted from PW cultivated in LCM-A and LCM-B

Parameter	LCM-A	LCM-B	ASTM 6751-12		EN 14214	
			Min	Max	Min	Max
Linolenic Acid (%wt)	0.66	0.17	-	-	-	12
Iodine Value (l)	63.8	60.3	-	-	-	120
Cetane number (l)	70	65.8	47	-	51	-
Oxidation Stability (hr)	7.4	13.4	6	-	8	-
Viscosity (mm ² s ⁻¹)	2.4	2.9	1.9	6	3.5	5
Density (kg m ⁻³)	0.6	0.7	-	-	0.86	0.9

When using the LCM-B, all the biodiesel parameters complies with the values prescribed by the ASTM standards. Moreover, most of the prescriptions of European regulation for quality biodiesel (EN 14214 and EN 590) are satisfied by the biodiesel obtained with LCM-B, except for slightly lower values of viscosity and density.

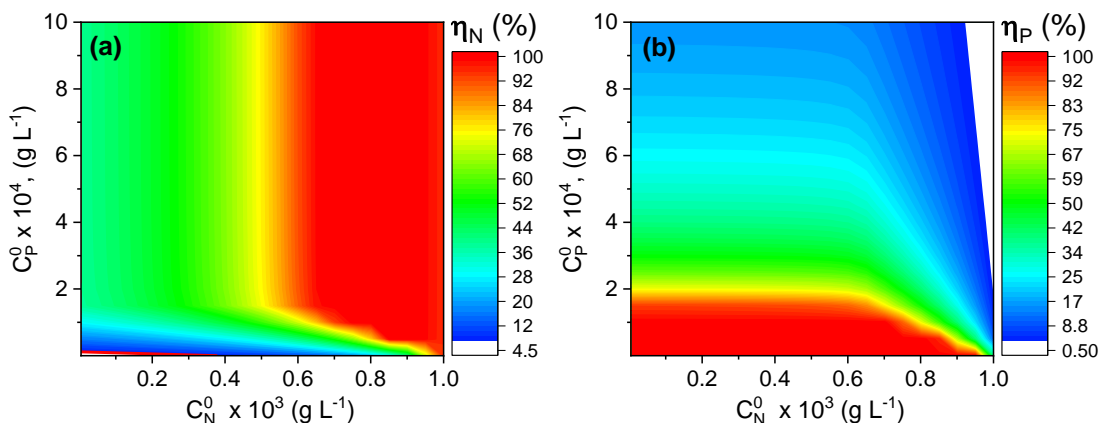


Figure 3. Effect of N and P initial concentrations on the removal rates of N (a) and P (b) after 560 h.

Therefore, it can be stated that the biodiesel obtained from PW cultivated with LCM-B would be of particularly good quality even without blending with fossil diesel. However, biodiesel produced by cultivating PW in LCM-A would not comply with the concerned standards even if the deviation from prescribed values is quite low for all the considered parameters.

Finally, to verify the potential capability of PW to remediate WW the model was run for different couples of values of initial concentration of N and P and then the corresponding remediation efficiencies achieved after 560 h of cultivation were evaluated (Fig. 3). All the other parameters and operating conditions were kept equal to the ones adopted in the experiments above described. The results of this simulation are summarized in Fig. 3 where it is shown that removal efficiencies close to 100% could be achieved for both N and P depending on the specific initial composition and thus on the specific WW being treated. In particular, N and P removal efficiencies equal to 20 and 8%, respectively were estimated when considering media with the same initial composition of LCM-A. The corresponding efficiencies were instead equal to about 80 and 70%, respectively, for media with the same N and P concentration of LCM-B.

Conclusions

Pseudochloris wilhelmii can be grown in mixtures of WWs and SW. Under specific operating conditions, the amount of lipid extracted from the alga was good with a FAMES composition that would allow producing a good quality biodiesel. The developed model, which well interpreted the experimental results, also allows extrapolating potentially good removal rates of N and P from LCM-B. Such information, while needing to be further validated by an investigation at the pilot scale, are encouraging in view of the profitable exploitation of PW at the large scale for the tertiary treatment of WWs through a process which permit obtaining biofuels.

References

- Abinandan S., Subashchandrabose S.R., Venkateswarlu K., Megharaj M., 2018, Nutrient removal and biomass production: advances in microalgal biotechnology for wastewater treatment, *Critical Reviews in Biotechnology*, 1–17.
- Concas A., Pisu M., Cao G., 2013, Mathematical Modelling of *Chlorella vulgaris* Growth in Semi-Batch Photobioreactors Fed with Pure CO₂, *Chemical Engineering Transactions*, 32, 1021-1026.
- Concas A., Pisu M., Cao G., 2016a, A novel mathematical model to simulate the size-structured growth of microalgae strains dividing by multiple fission, *Chemical Engineering Journal* 287, 252-268
- Concas, A., Lutz, G.A., Pisu, M., Cao, G., 2019, On the feasibility of *Pseudochloris wilhelmii* cultivation in sea-wastewater mixtures: modeling and experiments. *Journal of Environmental Chemical Engineering*, 7, 103031.
- Concas A., Malavasi V., Costelli C., Fadda P., Pisu M., Cao G., 2016b, Autotrophic growth and lipid production of *Chlorella sorokiniana* in lab batch and BIOCOIL photobioreactors: Experiments and modelling. *Bioresource Technology*, 211, 327–338.
- Ghangrekar, M. M., Shinde, V. B., 2006, Wastewater treatment in microbial fuel cell and electricity generation: A sustainable approach, In 12th international sustainable development research conference, 8, 201.
- Lutz G.A., Ciurli A., Chiellini C., Di Caprio F., Concas A., Dunford N.T., 2021, Latest developments in wastewater treatment and biopolymer production by microalgae, *Journal of Environmental Chemical Engineering*, 9 (1), 104926, <https://doi.org/10.1016/j.jece.2020.104926>.
- Lutz G.A., Concas A., Pisu M., Cao G., 2015, Batch growth kinetics of *Nannochloris eucaryotum* and its cultivation in semi-batch photobioreactors under 100% v/v CO₂: Experimental and modeling analysis, *Chemical Engineering Transactions* 43, 355-360.
- Lutz G.A., Locci A.M., Cao G., 2012, Effect of medium composition on the growth of *Nannochloris eucaryotum* in batch photobioreactors, *Journal of Biobased Materials and Bioenergy*, 6 94–100.
- Soru S., Malavasi V., Concas A., Caboni P., Cao G., 2018a, A novel investigation of the growth and lipid production of the extremophile microalga *Coccomyxa melkonianii* SCCA 048 under the effect of different cultivation conditions: Experiments and modelling, *Chemical Engineering Journal*, 377, 120589
- Tan Y., Wang Z.-X., Marshall K.C., 1998, Modeling pH effects on microbial growth: a statistical thermodynamic approach, *Biotechnology and Bioengineering*, 59, 724–731.
- Ummalyma S.B., Sukumaran R.K., Pandey A., 2018, Evaluation of Freshwater Microalgal Isolates for Growth and Oil Production in Seawater Medium, *Waste and Biomass Valorization*, 11, 223–230
- Wang Y.L., Yu S.L., Bao R.L., Yang J.Q., 2009, Treatment of Synthetic Wastewater by Combining Submerged MBR Technology and Aerobic Granular Technology, in: n 2009 3rd International Conference on Bioinformatics and Biomedical Engineering, 1-4.